Preprint Title	Smart DNA biosensor for in vitro detection of androgen receptor mRNA
Authors	Ekaterina A. Bryushkova, Erik R. Gandalipov and Julia V. Nuzhina
Publication Date	23 Jan 2020
Article Type	Full Research Paper
Supporting Information File 1	Bryushkova et al_2020_SI.docx; 206.8 KB
ORCID® iDs	Ekaterina A. Bryushkova - https://orcid.org/0000-0002-5227-114X; Julia V. Nuzhina - https://orcid.org/0000-0002-4863-9458

Smart DNA biosensor for in vitro detection of androgen receptor mRNA

Ekaterina A. Bryushkova[1]*, Erik R. Gandalipov[2], Julia V. Nuzhina[2]

[1]*Department of Molecular Biology, Lomonosov Moscow State University, Lenin Hills 1/12, Moscow, 119991, Russian Federation*

[2]*Laboratory of Solution Chemistry of Advanced Materials and Technologies, ITMO University, Lomonosova 9, St. Petersburg, 197101, Russian Federation*

**corresponding author: Ekaterina Alexandrovna Bryushkova, e.bryushkova@gmail.com*

Abstract

Local manifestations of hyperandrogenism are still difficult to diagnose since they are not associated with blood changes of androgens. An increase of androgen receptors (AR) expression level as much as their increase sensitivity to the corresponding ligands may lead to the manifestation of acne, androgenetic alopecia, or hirsutism. It means that in some cases an assessment of the local level of AR expression is necessary for the differential diagnosis and selects the relevant therapy. The traditional laboratory techniques are not available everywhere due to their complexity and laboriousness. In this project, a novel Smart DNA Biosensor, based on RNA-dependent split aptamer for the primary diagnosis of androgen receptors overexpression was developed. This molecular construction is easy to use, has high efficiency and selectivity, dui to its modular structure can be easily optimized for the detection of various targets. Thus, SDB-like sensors may be useful for the rapid differential diagnosis.

Keywords: DNA-based biosensor, androgen receptors, 10-23 deoxyribozymes, RNA cleavage, malachite green aptamer

Introduction

The term "hyperandrogenism" has become widespread in the scientific literature in the 21st century[1–4]. It usually means an increase in the effects of the androgen on the body, which may be the result of pathological hyperactivity of the endocrine glands[5], unbalanced conversion of steroids in the body[6] or excessive androgen receptor (AR) sensitivity to the corresponding ligands -

Androgen Insensitivity Syndrome[7]. For example, most women with idiopathic hirsutism have normal circulating adrenal and gonadal androgens[8]. Furthermore, AR oversensitivity can be associated both with highly selective ligand-receptor interaction and with an increase in the number of receptors on the surface of an individual cell. The consequences of hyperandrogenism can be extremely serious, ranging from local manifestations, such as androgenetic alopecia[9], adulthood acne or hirsutism[10], to impaired fat metabolism, muscle atrophy, irregular cycle in women and other metabolic disorders[11].

The androgen receptor (alternative name NR3C4) belongs to the steroid nuclear receptor superfamily, capable of being activated after a direct interaction with nuclear DNA, then transported into the nucleus and working as a transcription factor[12]. More than a hundred target genes of the androgen receptor are known, including genes encoding proteins involved in protein folding, secretion, intracellular signal transmission, proliferation, as well as differentiation and apoptosis[13]. Thus, the level of AR expression is an important diagnostic marker in various pathologies[14].

Laboratory diagnostic methods may easily detect systemic hyperandrogenism, however, the measurement of local androgens changes or AR expression is still a serious problem and requires the development of additional test systems. In modern biomedical diagnostics, different biosensors are being developed as a potential solution to these problems. Biosensors contain two main components: a biological recognition element (antibodies, enzymes, nucleic acid and other) that detects the target molecule, and a signalling component that converts the biological recognition into physically detectable signal. Since the early 1990s, DNA-based aptamers biosensors became widespread. Unlike proteins, DNA biosensors can be selected for any given target, including those without soliciting immune responses or with high toxicity. Also, these sensors can be easily synthesized outside living organisms, are smaller, more stable and can be repeatedly used without losing their binding capability[15,16]. DNA biosensors are typically used to detect nucleic acids,

proteins, amino acids, active forms or intermediate metabolites of hormones or drugs and other low molecular weight compounds[17].

A serious problem for detection of full-sized nucleic acids is the secondary structure, which interrupts the access of sensors to the binding site. When detecting single-stranded RNA, it was shown that this problem can be partially solved by adding additional sequences hybridizing with the target nucleic acid to the DNA biosensor design[18]. But in general, the problem of accessibility of the target nucleic acid site is still the main disadvantage of using DNA biosensors in this area.

In this project, we demonstrate an experimental model of smart DNA biosensor (SDB), designed to quickly and efficiently check the level of expression of the human AR. The design of SDB includes a number of functional advantages over most known biosensors and has the potential to solve the mentioned problem.

Results and Discussion

The human AR gene is located on the X chromosome at Xq11_12 and is encoded by eight exons. The first exon contains polymorphic CAG microsatellite repeats and codes for a variable length of the N-terminal domain (NTD). *In vitro* studies demonstrate that progressive expansion the length of CAG repeat in NTD may decrease its transactivation function. Exons 2 and 3 code for the central DNA-binding domain and exons 4 to 8 code for the C-terminal ligand-binding domain[19,20]. In different studies 18 alternative splice variants of AR mRNA - AR-FL, AR45, AR-23, AR V1-V14 and AR-8 - were described. Most of them encode a small-sized or functionally inactive proteins[21]. However, all translated isoforms of AR protein contain NTD, which is critical for AR function. Its modular activation function is important for both gene regulation and participation in protein-protein interactions[15]. This is the main reason to target our SDB construction against sequence inside the first exon.

Although splice variants of AR-FL (full-size molecule, alternative name AR1), AR-V7 (alternative name AR3) and AR-V9[22,23] are the most important for a clinical point of view, we

selected the target AR mRNA region using all nucleotide sequences of the translated AR mRNAs from open databases (Table S2, Fig.S1A). Then bioinformatics analysis of the human AR mRNA (Fig.S1B) was conducted using several evaluation criteria: (i) the target sequence should be found in the largest number of RNA transcripts of the AR gene, (ii) the target sequence should be specific only to the mRNA of the AR gene, (iii) the target sequence should possess low percentage of variability for single nucleotide polymorphisms. Based on the results of the bioinformatics analysis, an RNA sequence of 60 nt was selected (Table S2, 60-AR_RNA). This sequence is located in conserved exon 1, position 1–2140 nucleotides. The specificity of 60-AR_RNA for the human androgen receptor has been further verified using the BLAST algorithm (https://blast.ncbi.nlm.nih.gov/Blast.cgi).

The proposed SDB was developed with the purpose of facilitating the access of signaling component to the target sequence of AR mRNA. To do this, we chose an approach that increases the efficiency of the biosensor by cutting out a short sequence from mRNA, resulting in a more accessible secondary structure. Owing to better steric and thermodynamic conditions for nucleotide hybridization, we expected to see a significant increase in signal output for 60-nucleotide and 27-nucleotide sequences (Fig.1).

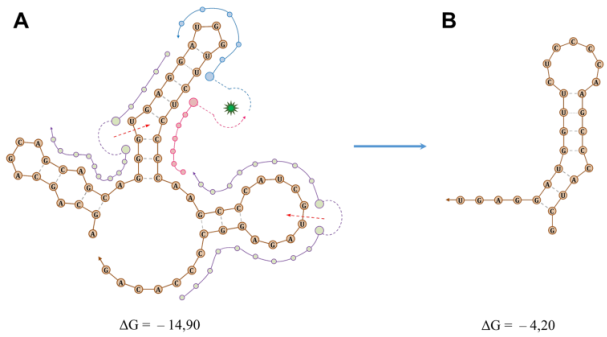

Figure 1: The theoretical predicted secondary structures of a target RNA before and after cleavage. A – an initial 60-nucleotide fragment of AR mRNA (60-AR_RNA); color lines indicate the possible orientation of SDB chains around RNA structure; red arrows indicate the assumed cleavage sites. B – a short 27-nucleotide fragment resulting from the 60-AR_RNA cleavage. A prediction of the RNA secondary structure with the folding energy before and after cleavage was performed by MFold open source

http://unafold.rna.albany.edu/?q=mfold/RNA-Folding-Form

We propose the model of SDB (Fig.2A) developed in our laboratory, which is based on the principles of Holliday junction and consists of several functional modules: (i) two catalytically active deoxyribozymes 10-23, (Dz1 and Dz2) hybridizes on both sides around the site of aptamer binding, (ii) biosensor with an aptameric signalling component, (iii) oligonucleotide platform, that

associate the components in a one united structure. A calculation of the SDB stability at physiological conditions was performed using the Nucleic Acid Package open service (http://www.nupack.org/).

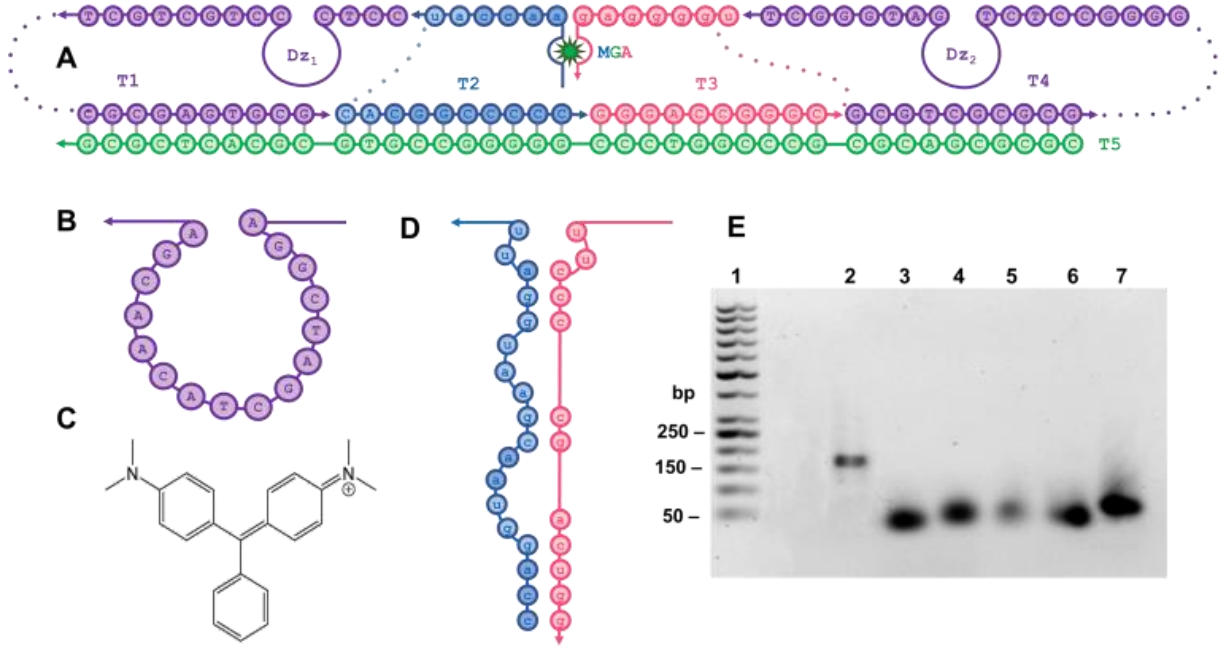

Figure 2: The SDB basic features. A - Schematic representation of the SDB structure. In T1 and T4 dotted lines indicate hexaethylene glycol linkers, in T2 and T3 - polythimidine linker; Dz1 and Dz2 — deoxyribozyme sequences. B - the detailed structure of Dz's catalytic center, cited by[24] with changes; green star indicates the malachite green dye. C - malachite green dye chemical structure. D - The detailed malachite green aptamer (MGA) structure with modifications. E - Confirmation of the biosensor assembly using agarose gel electrophoresis; lane 1: DNA ladder; lane 2: assembled SDB; Lanes 3–7: strands T1–T5 respectively.

Target mRNA cleavage was achieved using RNA-cleaving ability of Dz1 and Dz2 (Fig.S2) which are parts of T1 and T4 strands respectively. Biosensor part or signalling component is a modified split malachite green aptamer (MGA)[25] with additional RNA sequences, that are complementary to the target 60-AR_RNA (Fig.2A, T2 and T3 strands). MGA strands can hybridize with each other and bind a molecule of malachite green dye (Fig.2C and D) only in the presence of target mRNA and by this SDB is high specific sensor. Being bound in such structure, malachite

green dye can produce signal after excitation on 620 nm, which is detectable by fluorescence spectrophotometer.

All these sequences, T1–T4, also possess complementary to oligonucleotide platform (T5 strand) sites, joined to the strands by polythimidine or hexaethylene glycol linkers. These linkers provide more flexible binding to complete SDB.

Thus, we assumed that the cooperative work of both Dz1 and Dz2 allows an increase in the local concentration of short 28 nt fragments of the target mRNA near the MGA part of SDB, and DNA-core keeps all functional modules of the construction in close proximity. Sequences of the oligonucleotides used in the study are presented in Table S1. Complete SDB was assembled by annealing the individual component strands (T1–T5) to each other. The efficiency of SDB assembling was evaluated using agarose gel electrophoresis (Fig. 2E). The single band proves that in chosen conditions there is a complete hybridization of all 5 strands into an integrated SDB complex.

To estimate the functional activity of the developed molecule we simultaneously evaluate the biosensor fluorescence intensity and the efficiency of the target RNA cleavage in the presence of SDB under the same conditions. Complete assembled SDB (100 nM), mix of T1–T5 (100 nM each strand) without annealing and mix of T2-T3 (100 nM for each chain) with integrated MGA also without annealing were incubated for 6 hrs in a buffer at 37°C with 60-AR_RNA (fluorescence assay) or FAM-60-AR_RNA (cleavage assay). All fluorescence samples and one of the samples with SDB and FAM-ADR_RNA contained 25 μM malachite green dye. As a negative control samples with only 60-AR_RNA or FAM-60-AR_RNA were incubated in the same conditions. After incubation fluorescence measurement was conducted by fluorescence spectrophotometry (620/648 nm) (Fig.3A) and cleavage was verified by denaturing PAAG (Fig.3B).

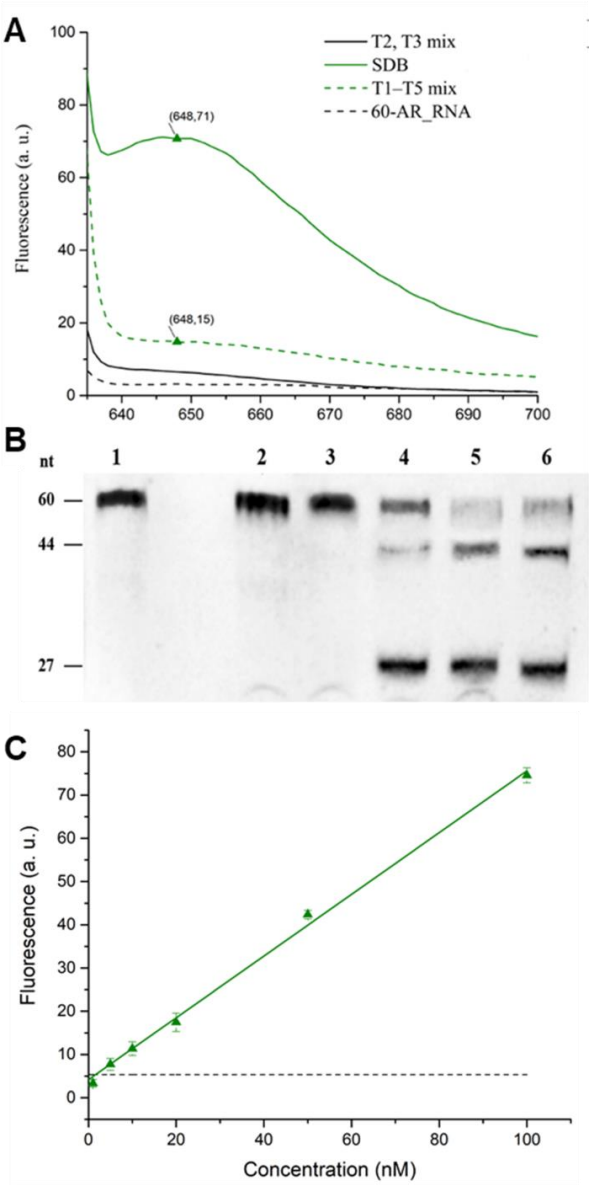

Figure 3: The SDB functional activity A – emission spectra of assembled SDB (green line), T1–T5 chains mix without annealing (green dotted line), aptamer sample containing chains T2 and T3 (black dotted line) and a control sample with 60-AR_RNA (black line) after 6 hrs of incubation. B – denaturing PAGE assessment of cleavage of samples containing 60-FAM-AR_RNA and different agents after 6 hrs incubation; lanes 1 and 2: 60-FAM-AR_RNA incubated for 0 hours and 6 hours respectively; lane 3: 60-FAM-AR_RNA, T2 and T3; lane 4: 60-FAM-AR_RNA and individual strands T1–T5; lane 5: 60-FAM-AR_RNA with assembled SDB; lane 6: 60-FAM-AR_RNA with assembled SDB in the presence of malachite green dye. C – limit of detection for SDB. Each dot is an average of triplicate values of fluorescence for samples with different concentrations of 60-AR_RNA; standard deviations are shown. Green line is a linear regression line for these dots. Dash line indicates the threshold value of fluorescence of buffer with malachite green dye.

According to densitometry analysis, around 90% of FAM-60-AR_RNA is cleaved by one or both deoxyribozymes in the composition of complete SDB, and 70% is cleaved by mixture of separate T1–T5 strands. Farther, the intensity of the fluorescent signal in the sample containing the assembled SDB with 60-AR_RNA was 10 times higher than the signal of samples containing individual MGA strands (T2 and T3 mix), and 5 times higher than the signal from samples containing unassembled SDB strains (Fig.3A, T1–T5 mix). These results seem to confirm our hypothesis on facilitating the ease of access to target RNA by cutting a short 27-nt fragment from the full target sequence (Fig.3B) thus increasing the local concentration of this fragment near the

sensing part of SDB. As follows from Fig.2B (line 6), the presence of malachite green dye does not affect the catalytic activity of SDB.

The next step was to assess the limit of detection (LOD) of the biosensor we developed. For this experiment, samples containing 100 nM of annealed SDB and 25 μM of malachite green dye in the same buffer were incubated with different amounts of 60-AR_RNA (1 nM, 5 nM, 10 nM, 20 nM, 50 nM, 100 nM) for 6 hours at 37°C. Then the fluorescence of the samples was measured and LOD was calculated. According to the data obtained, the LOD of the DNA nanostructure we developed is 1.6 nM (Fig.3C), and that value is near to the minimum LOD described for the MGA.

Experimental

For detailed experimental description please see Supporting Information File

Conclusions

In conclusion, we developed a modular DNA biosensor for the primary diagnosis of AR overexpression. On a model system SDB demonstrated its high functional activity, as well as specificity for the selected target sequence. On the one hand, the complex SDB molecule has a catalytic advantage over free deoxyribozymes, and on the other hand, it circumvents the limitations imposed on the biosensor by the secondary structure of the target nucleic acid. The traditional laboratory techniques (such as PCR and RT-PCR) are often not available due to their complexity and laboriousness. Easy to use and easily optimized for any target molecule, SDB can be very convenient for use in conditions of rapid field diagnostics.

The next step in this work will be the extrapolation of the results to full-sized AR mRNA and optimization of the SDB on biological material.

Acknowledgements

Authors thank the Professor Dmitry M Kolpashchikov from University of Central Florida for the inspiration, coordination and participation in the discussion of this project.

Funding

This work was supported by RFBR grant # 18-34-00898 mol_a

Conflicts of interest

The authors declare no competing financial or other interests.

Authors' contribution: Bryushkova E.A., Gandalipov E.R. and Nuzhina J.V. performed the experiments; Bryushkova E.A. supervised the students and planned the experiments; all authors analyzed the data, and wrote the article.

Notes and references

1 Hernandez, M. I.; López, P.; Gaete, X.; Villarroel, C.; Cavada, G.; Avila, A.; Iñiguez, G.; Cassorla, F. Hyperandrogenism in Adolescent Girls: Relationship with the Somatotrophic Axis. *J. Pediatr. Endocrinol. Metab.* **2017**, *30* (5), 561–568. https://doi.org/10.1515/jpem-2016-0340.

2 Karnath B.M. Signs of Hyperandrogenism in Women. *Hosp. Physician* **2008**, *4* (10), 25–30.

3 Peigné, M.; Villers-Capelle, A.; Robin, G.; Dewailly, D. Hyperandrogénie Féminine. *Presse Medicale*. November 2013, pp 1487–1499. https://doi.org/10.1016/j.lpm.2013.07.016.

4 Yildiz, B. O. Diagnosis of Hyperandrogenism: Clinical Criteria. *Best Practice and Research: Clinical Endocrinology and Metabolism*. June 2006, pp 167–176. https://doi.org/10.1016/j.beem.2006.02.004.

5 Alali, I.; Haj Hassan, L.; Mardini, G.; Hijazi, N.; Hadid, L.; Kabalan, Y. Diagnostic Dilemma in Two Cases of Hyperandrogenism. *Case Rep. Endocrinol.* **2018**, *2018*, 1–4. https://doi.org/10.1155/2018/9041018.

6 Rachoń, D. Differential Diagnosis of Hyperandrogenism in Women with Polycystic Ovary Syndrome. *Experimental and Clinical Endocrinology and Diabetes*. 2012, pp 205–209. https://doi.org/10.1055/s-0031-1299765.

7 Galani, A.; Kitsiou-Tzeli, S.; Sofokleous, C.; Kanavakis, E.; Kalpini-Mavrou, A. Androgen Insensitivity Syndrome: Clinical Features and Molecular Defects. *Hormones*. Hellenic Endocrine Society 2008, pp 217–229. https://doi.org/10.14310/horm.2002.1201.

8 Vottero, A.; Stratakis, C. A.; Ghizzoni, L.; Longui, C. A.; Karl, M.; Chrousos, G. P. Androgen Receptor-Mediated Hypersensitivity to Androgens in Women with Nonhyperandrogenic Hirsutism: Skewing of X-Chromosome Inactivation [1]. *J. Clin. Endocrinol. Metab.* **1999**, *84* (3), 1091–1095. https://doi.org/10.1210/jcem.84.3.5540.

9 Richeti, F.; Kochi, C.; Rocha, M. N.; Sant'anna Corrêa, C.; Lazzarini, R.; Guazzelli, R. M.; Mendonça, R. F.; Melo, M. R.; Longui, C. A. Increased Androgen Receptor Messenger RNA in Frontal-Parietal Hair Follicles of Women with Androgenetic Alopecia. *Genet. Mol. Res.* **2013**, *12* (2), 1834–1840. https://doi.org/10.4238/2013.February.28.19.

10 Raab Univ Wolfgang Raab, P. Skin Diseases Due to Increased Androgen Sensitivity. *J. Appl Cosmetol* **1999**, *17*, 23–35.

11 Zhang, B.; Wang, J.; Shen, S.; Liu, J.; Sun, J.; Gu, T.; Ye, X.; Zhu, D.; Bi, Y. Association of Androgen Excess with Glucose Intolerance in Women with Polycystic Ovary Syndrome. *Biomed Res. Int.* **2018**, *2018*. https://doi.org/10.1155/2018/6869705.

12 Mooradian, A. D.; Morley, J. E.; Korenman, S. G. Biological Actions of Androgens. *Endocr. Rev.* **1987**, *8* (1), 1–28. https://doi.org/10.1210/edrv-8-1-1.

13 McEwan, I. J. Molecular Mechanisms of Androgen Receptor-Mediated Gene Regulation: Structure-Function Analysis of the AF-1 Domain. *Endocrine-Related Cancer*. June 2004, pp 281–293. https://doi.org/10.1677/erc.0.0110281.

14 Elattar, A.; Warburton, K. G.; Mukhopadhyay, A.; Freer, R. M.; Shaheen, F.; Cross, P.; Plummer, E. R.; Robson, C. N.; Edmondson, R. J. Androgen Receptor Expression Is a Biological Marker for Androgen Sensitivity in High Grade Serous Epithelial Ovarian Cancer. *Gynecol. Oncol.* **2012**, *124* (1), 142–147. https://doi.org/10.1016/j.ygyno.2011.09.004.

15 Wach, S.; Taubert, H.; Cronauer, M. Role of Androgen Receptor Splice Variants, Their Clinical Relevance and Treatment Options. *World J. Urol.* **2019**. https://doi.org/10.1007/s00345-018-02619-0.

16 Zhou, W.; Jimmy Huang, P. J.; Ding, J.; Liu, J. Aptamer-Based Biosensors for Biomedical Diagnostics. *Analyst*. May 6, 2014, pp 2627–2640. https://doi.org/10.1039/c4an00132j.

17 E. Wang, R.; Zhang, Y.; Cai, J.; Cai, W.; Gao, T. Aptamer-Based Fluorescent Biosensors. *Curr. Med. Chem.* **2011**, *18* (27), 4175–4184. https://doi.org/10.2174/092986711797189637.

18 Cox, A. J.; Bengtson, H. N.; Gerasimova, Y. V.; Rohde, K. H.; Kolpashchikov, D. M. DNA Antenna Tile-Associated Deoxyribozyme Sensor with Improved Sensitivity. *ChemBioChem* **2016**, *17* (21), 2038–2041. https://doi.org/10.1002/cbic.201600438.

19 Gelmann, E. P. Molecular Biology of the Androgen Receptor. *Journal of Clinical Oncology*. July 1, 2002, pp 3001–3015. https://doi.org/10.1200/JCO.2002.10.018.

20 MacLean, H. E.; Warne, G. L.; Zajac, J. D. Localization of Functional Domains in the Androgen Receptor. *J. Steroid Biochem. Mol. Biol.* **1997**, *62* (4), 233–242. https://doi.org/10.1016/s0960-0760(97)00049-6.

21 Lu, C.; Luo, J. Decoding the Androgen Receptor Splice Variants. *Translational Andrology and Urology*. AME Publishing Company 2013, pp 178–186. https://doi.org/10.3978/j.issn.2223-4683.2013.09.08.

22 Guo, Z.; Qiu, Y. A New Trick of an Old Molecule: Androgen Receptor Splice Variants Taking the Stage?! *International Journal of Biological Sciences*. Ivyspring International Publisher 2011, pp 815–822. https://doi.org/10.7150/ijbs.7.815.

23 Kallio, H. M. L.; Hieta, R.; Latonen, L.; Brofeldt, A.; Annala, M.; Kivinummi, K.; Tammela, T. L.; Nykter, M.; Isaacs, W. B.; Lilja, H. G.; et al. Constitutively Active Androgen Receptor Splice Variants AR-V3, AR-V7 and AR-V9 Are Co-Expressed in Castration-Resistant Prostate Cancer Metastases. *Br. J. Cancer* **2018**, *119* (3), 347–356. https://doi.org/10.1038/s41416-018-0172-0.

24 Silverman, S. K. Catalytic DNA: Scope, Applications, and Biochemistry of Deoxyribozymes. *Trends in Biochemical Sciences*. Elsevier Ltd July 1, 2016, pp 595–609. https://doi.org/10.1016/j.tibs.2016.04.010.

25 Kolpashchikov, D. M. Binary Malachite Green Aptamer for Fluorescent Detection of Nucleic Acids. *J. Am. Chem. Soc.* **2005**, *127* (36), 12442–12443. https://doi.org/10.1021/ja0529788.